Supplementary Material to: The effect of mixed termination composition in Sc, Ti, and V-based MXenes

Michal Novotný,[*] Karolína Tkáčová,[*] František Karlický[*]

August 7, 2024

[*]Department of Physics, Faculty of Science, University of Ostrava, 30. dubna 22, 701 03 Ostrava, Czech Republic, frantisek.karlicky@osu.cz

1 K-point downsampling

While the energy differences may indicate that a 2×2×1 grid would be sufficient, this sparse grid produced an indirect band gap of 0.154 eV while denser grids predict the system to be metallic both for PBE and SCAN density functionals. In our methodology, we first pre-converge the wave function using the PBE functional and then use this as a starting point for the SCAN calculation. Using denser k-point grids for PBE has not yielded better results or faster convergence of the SCAN calculations, quite the opposite the reading of the wave function can lead to significant slowdowns with dense k-point grids. We have therefore chosen to use a 2×2×1 k-point grid for PBE and 3×3×1 grid for SCAN for all subsequent calculations of 3×3 cells.

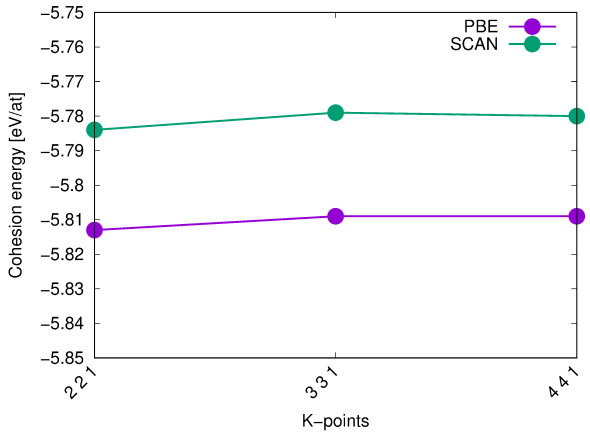

Figure S1: K-point convergence of cohesion energy. The test was performed on a 3×3 cell with a mirrored coverage of $Sc_2CF_{0.33}O_{0.45}(OH)_{0.22}$

2 Weighted average lattice constants

Table S1: Evaluation of weighted average (WA) lattice constants compared to relaxed supercells for three distinct Sc-MXene coverages in 3×3 supercell. The patterns were mirrored on both sides. The strain was calculated as a ratio of the WA lattice constant to the fully relaxed one. The atomic displacements were calculated as the difference in atomic positions between the WA after atomic relaxation and fully relaxed suppercell.

Coverage	External pressure [kB]		Strain	Largest atomic displacement [Å]			Cohesion Energy [eV/atom]	
	Relaxed	WA	[%]	X	Y	Z	Relaxed	WA
Before relaxation of atomic positions								
$Sc_2CF_{0.33}O_{0.22}(OH)_{0.45}$	1.4	-0.75	-0.27	0.116	0.121	0.211	-5.763	-5.689
$Sc_2CF_{0.33}O_{0.33}(OH)_{0.34}$	0.44	-1.7	-0.35	0.075	0.080	0.221	-5.867	-5.738
$Sc_{0.45}CF_{0.22}O_{0.33}(OH)_{0.45}$	0.06	-2.25	-0.35	0.063	0.061	0.226	-5.965	-5.827
After relaxation of atomic positions								
$Sc_2CF_{0.33}O_{0.22}(OH)_{0.45}$	1.4	-0.75	-0.27	10^{-5}	10^{-5}	0.001	-5.763	-5.733
$Sc_2CF_{0.33}O_{0.33}(OH)_{0.34}$	0.44	-1.7	-0.35	10^{-6}	10^{-5}	0.001	-5.867	-5.848
$Sc_{0.45}CF_{0.22}O_{0.33}(OH)_{0.45}$	0.06	-2.25	-0.35	10^{-4}	10^{-6}	0.002	-5.965	-5.901

3 MXenes with single type of surface termination

Table S2: Bond dissociation energies for F, O, and OH terminal groups from a 3×3 M_2CTT' supercell, where T denotes terminal groups on the top of the MXene and T' on the bottom. μ indicates the pre-set magnetic state of the structure with the T-group vacancy.

Coverage	Dissociated	Sc			Ti			V		
TT'	bond	0 μ_B	1 μ_B	2 μ_B	0 μ_B	1 μ_B	2 μ_B	0 μ_B	1 μ_B	2 μ_B
FF	-F	-7.78	-7.46	-	-7.78	-7.46	-	-5.64	-5.18	-
OF	-F	-7.52	-6.99	-7.08	-7.52	-6.99	-7.08	-6.55	-6.51	-6.56
(OH)F	-F	-6.77	-6.52	-	-6.77	-6.52	-	-5.16	-4.96	-
OO	-O	-7.18	-6.85	-6.82	-7.18	-6.85	-6.82	-6.83	-6.69	-6.63
FO	-O	-6.55	-6.03	-	-6.55	-6.03	-	-5.20	-5.15	-
(OH)O	-O	-6.89	-6.57	-	-6.89	-6.57	-	-5.13	-5.20	-
(OH)(OH)	-OH	-7.72	-7.45	-	-7.72	-7.45	-	-5.64	-5.42	-
F(OH)	-OH	-5.99	-5.49	-	-5.99	-5.49	-	-4.71	-4.69	-
O(OH)	-OH	-7.40	-6.99	-7.04	-7.40	-6.99	-7.04	-6.81	-6.74	-6.69

4 MXenes with mixed surface termination

To describe patterns of terminal groups we chose to represent them by a code corresponding to their position on the surface of the MXene going by row from bottom to top and by row from left to right. For recognizability, the (OH) group is represented by the symbol **H**. The positions of t-groups in the pattern code are shown in Fig. S2.

Table S3: Cohesion energies and band gaps of 3×3 Sc_2CT_2 with mirrored pattern on both sides but shifted and/or rotated with respect to each other.

Top pattern 123456789	Bottom pattern 123456789	E_{coh} [eV/at]	Gap direct [eV]	Gap indirect [eV]
HHOFOOOFF	HHOFOOOFF	-5.7784	0	0
	OFFHHOFOO	-5.7801	0	0
	OHHOFOFOF	-5.7786	0	0
	OOFHOFHFO	-5.7762	0	0
HOHOHFFFF	HOHOHFFFF	-5.7749	0	0
	OHFFFFHOH	-5.775	0	0
	FOHFHOFHF	-5.772	0	0
	HOHFFFFHO	-5.7747	0	0
	OHFHOFFHF	-5.7722	0	0
	FHOFFHFOH	-5.7716	0	0
	HFFHFOOFH	-5.7732	0	0
FHHHHFHFF	FHHHHFHFF	-5.6303	0.991	0.831
	HFFFHHHHF	-5.6303	0.991	0.831
	HFHFHHFHF	-5.6303	0.991	0.831
	HFFHHFFHH	-5.6294	0.986	0.828
	HHFHFFFHH	-5.6303	0.991	0.831
	FHFHFHHHF	-5.6294	0.989	0.828
	HFHFHFHHF	-5.6303	0.99	0.831
	HHFFHHFFH	-5.6294	0.986	0.827
	FHFFHHHFH	-5.6294	0.989	0.827
	FHFHFHFHH	-5.6303	0.991	0.831
HHHFFFFFF	HHHFFFFFF	-5.8108	1.027	0.937
	FFFHHHFFF	-5.8109	1.018	0.932
	HFFHFFHFF	-5.8108	1.032	0.94
	FFFFFFHHH	-5.8109	1.034	0.94
	FHFFHFFHF	-5.8108	1.032	0.939
	FFHFFHFFH	-5.8109	1.032	0.94

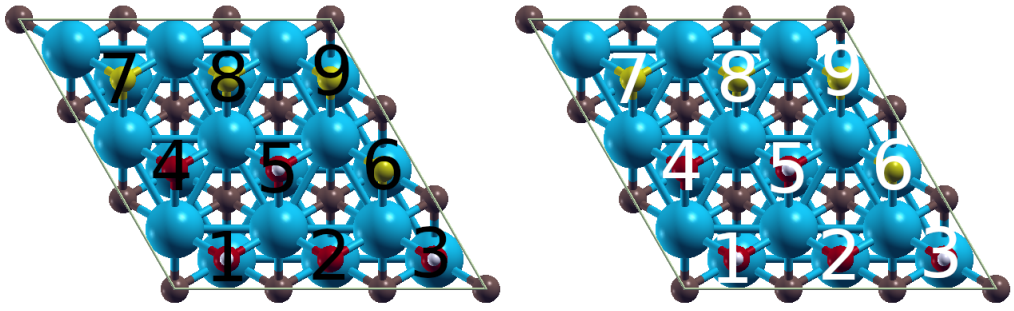

Figure S2: Terminal group positions in the surface pattern.

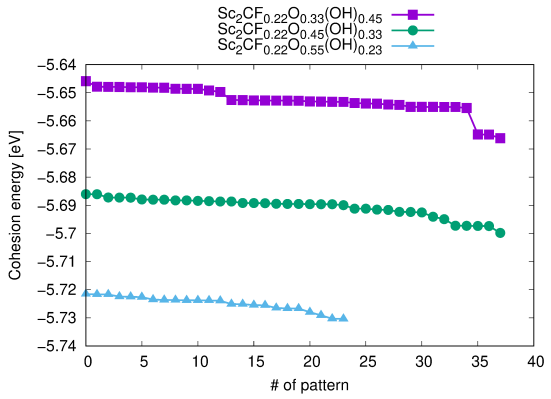

Figure S3: Cohesion energy of specific T-group concentrations with varying chemically distinct patterns.

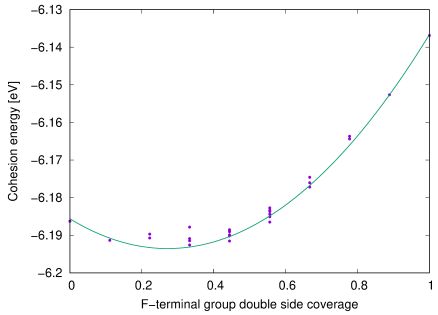

Figure S4: Cohesion energy of $Sc_2CF_{2c}O_{2(1-c)}$ as a function of single side F-group coverage c.

Table S4: Cohesion energies of MXenes M_2CTT', where M/T denotes terminal groups on the top of the MXene and M'/T' on the bottom, with sides fully covered by one terminal group.

Coverage	E_{coh} [eV/atom]		
TT'	Sc	Ti	V
FF	-6.14	-6.28	-5.72
OO	-6.19	-6.92	-6.27
OHOH	-5.34	-5.51	-5.14
FO	-6.13	-6.57	-6.00
FOH	-5.68	-5.83	-5.38
OOH	-5.67	-6.08	-5.61

5 Band structures and band gaps

Figure S5: Atomically resolved band structures of Sc-based MXenes, which embody conductive transition due to the inclusion of O-terminal groups. The Fermi level was set to 0. Red circles correspond to band contributions from Sc atoms, green from F atoms, blue from O atoms in OH, and yellow from O-terminations. The size of the dots corresponds to the spectral contributions of the atomic species to the band as outlined by Popescu et al.[1]

Table S5: Band gap of $Sc_2CF_{2c}(OH)_{2(1-c)}$ as a function of F-group coverage ($0 \leq c \leq 1$) represented as a fraction of the number of F-terminal groups to all available sites. The table shows the process of substituting OH groups by F-terminations on both sides with identical patterns on both sides. We include all available chemically distinct terminal group patterns for a given $F_{2c}(OH)_{2(1-c)}$ composition.

Double-sided F-group coverage	Top pattern 123456789	Bottom pattern 123456789	Gap direct [eV]	Gap indirect [eV]
0.00	HHHHHHHHH	HHHHHHHHH	0.499	0.499
0.22	FHHHHHHHH	FHHHHHHHH	0.869	0.869
0.44	FFHHHHHHH	FFHHHHHHH	1.219	0.903
0.44	HHHHFHHHF	HHHHFHHHF	1.211	0.906
0.67	FFFHHHHHH	FFFHHHHHH	1.368	0.926
0.67	FHHHFHHHF	FHHHFHHHF	1.311	0.919
0.67	HHHFHHHFF	HHHFHHHFF	1.359	0.920
0.67	HHHHHFHFF	HHHHHFHFF	1.369	0.932
0.89	FFFFHHHHH	FFFFHHHHH	1.379	0.938
0.89	FHHFHHHFF	FHHFHHHFF	1.382	0.942
0.89	FHHHHFHFF	FHHHHFHFF	1.386	0.949
0.89	HFHHHFHFF	HFHHHFHFF	1.376	0.942
0.89	HHHFHFHFF	HHHFHFHFF	1.376	0.939
0.89	HHHHFFHFF	HHHHFFHFF	1.402	0.961
1.11	FFFFFHHHH	FFFFFHHHH	1.404	0.961
1.11	FHHHFFHFF	FHHHFFHFF	1.405	0.964
1.11	FHHHHFFFF	FHHHHFFFF	1.404	0.965
1.11	HFHFHFHFF	HFHFHFHFF	1.413	0.976
1.11	HFHHHFFFF	HFHHHFFFF	1.406	0.964
1.11	HHFHHFFFF	HHFHHFFFF	1.406	0.966
1.33	FFFFFFHHH	FFFFFFHHH	1.442	0.996
1.33	FFHFHFHFF	FFHFHFHFF	1.436	0.998
1.33	FHHHFFFFF	FHHHFFFFF	1.424	0.982
1.33	HHFHFFFFF	HHFHFFFFF	1.439	0.996
1.56	FFFFFFFHH	FFFFFFFHH	1.455	1.009
1.56	FHFHFFFFF	FHFHFFFFF	1.462	1.017
1.78	FFFFFFFFH	FFFFFFFFH	1.483	1.032
2.00	FFFFFFFFF	FFFFFFFFF	1.507	1.061

Table S6: Band gap of $Sc_2CF_{2c}(OH)_{2(1-c)}$ as a function of F-group coverage ($0 \leq c \leq 1$) represented as a fraction of the number of F-terminal groups to all available sites. The table shows the process of substituting OH groups by F-terminations first on side until saturation and then on the other side. We include all available chemically distinct terminal group patters for a given $F_{2c}(OH)_{2(1-c)}$ composition.

Double sided F-group coverage	Top pattern 123456789	Bottom pattern 123456789	Gap direct [eV]	Gap indirect [eV]
0.00	HHHHHHHHH	HHHHHHHHH	0.499	0.499
0.12	HHHHHHHHH	FHHHHHHHH	0.591	0.591
0.22	HHHHFHHHF	HHHHHHHHH	0.620	0.62
0.22	HHHHHHHHH	FFHHHHHHH	0.625	0.625
0.34	FHHHFHHHF	HHHHHHHHH	0.651	0.651
0.34	HHHFHHHFF	HHHHHHHHH	0.666	0.666
0.34	HHHHHFHFF	HHHHHHHHH	0.666	0.666
0.34	HHHHHHHHH	FFFHHHHHH	0.657	0.657
0.44	FHHFHHHFF	HHHHHHHHH	0.694	0.694
0.44	FHHHHFHFF	HHHHHHHHH	0.709	0.709
0.44	HFHHHFHFF	HHHHHHHHH	0.697	0.697
0.44	HHHFHFHFF	HHHHHHHHH	0.703	0.703
0.44	HHHHFFHFF	HHHHHHHHH	0.695	0.695
0.44	HHHHHHHHH	FFFFHHHHH	0.693	0.693
0.56	FHHHFFHFF	HHHHHHHHH	0.730	0.73
0.56	FHHHHFFFF	HHHHHHHHH	0.719	0.719
0.56	HFHFHFHFF	HHHHHHHHH	0.728	0.728
0.56	HFHHHFFFF	HHHHHHHHH	0.734	0.734
0.56	HHFHHFFFF	HHHHHHHHH	0.740	0.74
0.56	HHHHHHHHH	FFFFFHHHH	0.731	0.731
0.66	FFHFHFHFF	HHHHHHHHH	0.786	0.786
0.66	FHHHFFFFF	HHHHHHHHH	0.755	0.755
0.66	HHFHFFFFF	HHHHHHHHH	0.775	0.775
0.66	HHHHHHHHH	FFFFFFHHH	0.762	0.762
0.78	FHFHFFFFF	HHHHHHHHH	0.814	0.814
0.78	HHHHHHHHH	FFFFFFFHH	0.797	0.797
0.88	HHHHHHHHH	FFFFFFFFH	0.850	0.85
1.00	HHHHHHHHH	FFFFFFFFF	0.856	0.856
1.12	FHHHHHHHH	FFFFFFFFF	1.208	0.979
1.22	FFHHHHHHH	FFFFFFFFF	1.383	0.98
1.22	HHHHFHHHF	FFFFFFFFF	1.381	0.983
1.34	FFFHHHHHH	FFFFFFFFF	1.430	0.983
1.34	FHHHFHHHF	FFFFFFFFF	1.442	0.99
1.34	HHHFHHHFF	FFFFFFFFF	1.432	0.986
1.34	HHHHHFHFF	FFFFFFFFF	1.436	0.991
1.44	FFFFHHHHH	FFFFFFFFF	1.443	0.997
1.44	FHHFHHHFF	FFFFFFFFF	1.450	1.002
1.44	FHHHHFHFF	FFFFFFFFF	1.445	1.005
1.44	HFHHHFHFF	FFFFFFFFF	1.438	0.995
1.44	HHHFHFHFF	FFFFFFFFF	1.444	1.001
1.44	HHHHFFHFF	FFFFFFFFF	1.453	1.004
1.56	FFFFFHHHH	FFFFFFFFF	1.457	1.01
1.56	FHHHFFHFF	FFFFFFFFF	1.461	1.012
1.56	FHHHHFFFF	FFFFFFFFF	1.458	1.011
1.56	HFHFHFHFF	FFFFFFFFF	1.455	1.011
1.56	HFHHHFFFF	FFFFFFFFF	1.447	0.999
1.56	HHFHHFFFF	FFFFFFFFF	1.458	1.011
1.66	FFFFFFHHH	FFFFFFFFF	1.467	1.016
1.66	FFHFHFHFF	FFFFFFFFF	1.464	1.024
1.66	FHHHFFFFF	FFFFFFFFF	1.463	1.014
1.66	HHFHFFFFF	FFFFFFFFF	1.468	1.021
1.78	FFFFFFFHH	FFFFFFFFF	1.473	1.026
1.78	FHFHFFFFF	FFFFFFFFF	1.477	1.034
1.88	FFFFFFFFH	FFFFFFFFF	1.489	1.042
2.00	FFFFFFFFF	FFFFFFFFF	1.507	1.061

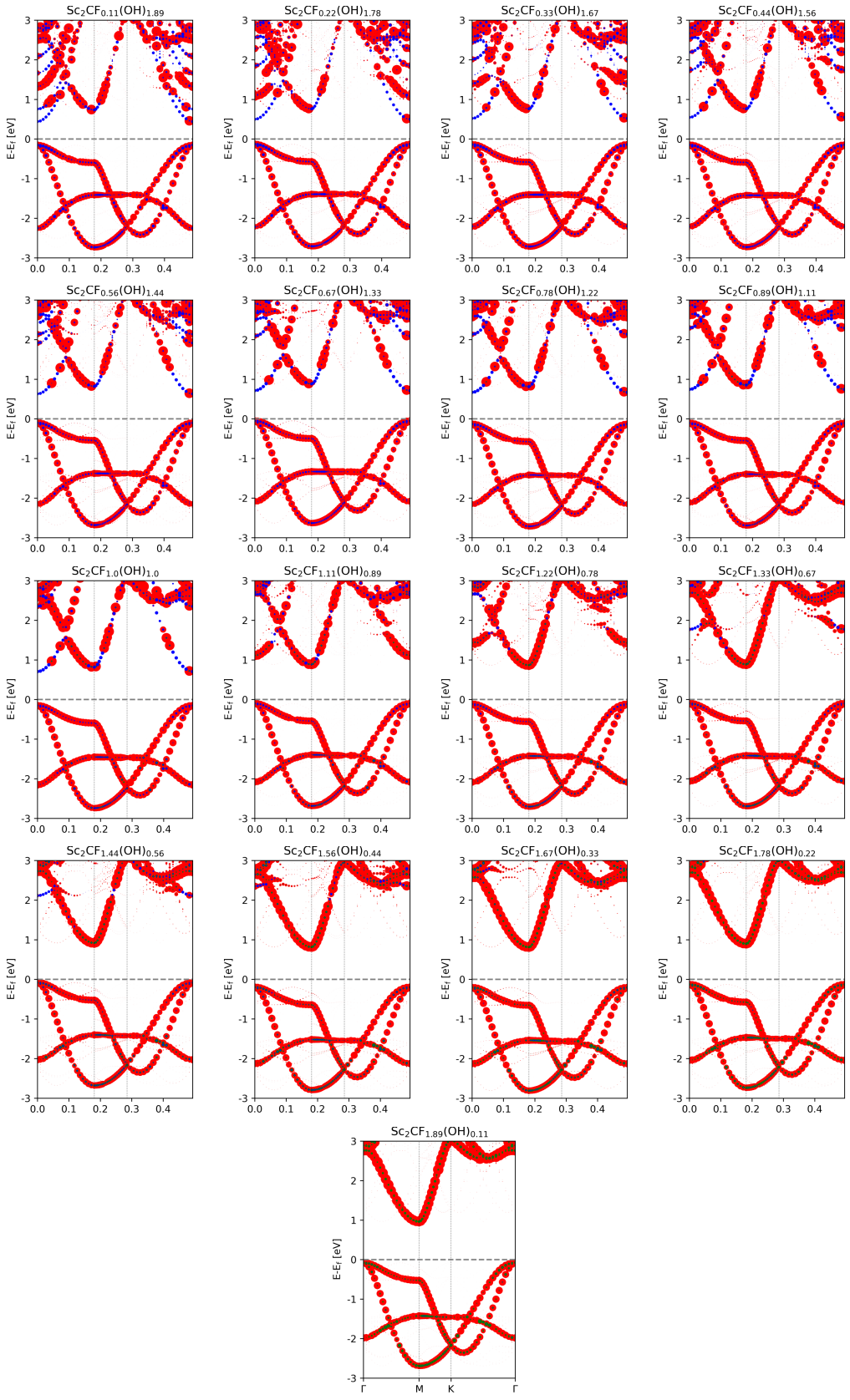

Figure S6: Band structures of Sc-based MXenes. Details as in Figure 4 of the main text.

References

1. V. Popescu and A. Zunger, *Physical Review B*, 2012, **85**, 085201.